HEFAT2012
9th International Conference on Heat Transfer, Fluid Mechanics and Thermodynamics
16 – 18 July 2012
Malta

Study of Atmospheric Ice Accretion on Onshore Structures using CFD Based Numerical Approach

Muhammad S. Virk
High North Technology Centre
Department of Technology
Narvik University College, 8505 Narvik, Norway
Email: msv@hin.no

ABSTRACT

Atmospheric ice accretion occurs, when super cooled water droplets come into contact with the exposed surface of a structure in cold regions like arctic and alpine. Most investigations of this subject have been performed using experimental techniques, but for the last decade or so the computational fluid dynamics (CFD) based numerical techniques have begun to play a significant role in understanding and simulating the atmospheric ice accretion on structures. This research work highlights the application of CFD in field of atmospheric ice accretion and describes the CFD based numerical analyses of atmospheric ice accretion on various on-shore structures such as wind turbine blades, circular overhead power line conductors and building's air intake louvers. Numerical results of this research work are compared with the experimental data to validate and a good agreement is found.

INTRODUCTION

Human activities are increasingly extending to the cold climate regions, where atmospheric icing not only create human inconvenience, but also affect human activities especially in the construction industry (*communication towers and ski lifts)*, energy distribution (*power network cables and towers*), aviation conditions on the ground, meteorological observations and wind energy power production. Various onshore structures have been damaged or destroyed due to the added mass of ice or an increase in aerodynamic interaction leading to unacceptable movements [1]. Therefore good understanding atmospheric icing physics and accretion rate is crucial for the design of safe structures in cold regions.

Water droplets in the earth atmosphere can remain in the liquid state at air temperature as low as -40 ^{o} C, before spontaneous freezing occurs [2, 3]. The rate of atmospheric ice accretion on a structure is governed by two processes; the impingement of super cooled water droplets on the structure surface and the surface thermodynamics, which determines that what portion of the water impingement freezes or on other hand melts previously accreted ice. Numerical study of atmospheric ice accretion on structures includes the computation of mass flux of icing particles as well as determination of the icing conditions [4]. This can be numerically simulated by means of integrated thermo-fluid dynamic models, which requires the use of various numerical tools in order to obtain the flow field, the particle behavior, surface thermodynamic and phase change. Various numerical studies related to the atmospheric icing on structures can be found in literature from late 1970's, where researchers such as Ackley and Templeton [5], Lozowski and Oleskiw [6-8], McComber et al. [9, 10], Smith and Barker [11] has concentrated on understanding the physical ice accretion processes and developing numerical models to predict the severity of icing on structures. During 1990's Makkonen [12, 13], Finstad et al. [14], Shin et al. [15-17] & Skelton et al. [18] worked on numerical modeling of the atmospheric ice accretion. This paper highlights the application of CFD for 2D and 3D numerical study of atmospheric ice accretion on various onshore structures such as wind turbine blades, overhead circular power line conductors and building's air intake louvers. A detailed parametric study at Narvik University College is carried out to understand the effect of various operating and geometric conditions on rate and shape of atmospheric ice accretion on these structures.

METHODOLOGY

Numerical modeling of atmospheric icing is a complex coupled process that involves the fluid flow simulation, droplet behavior, surface thermodynamics and phase change. In this study numerical analyses were carried out using a finite element based Navier-Stoke equation solver 'FENSAPICE' from NTI [19] and Fluent from ANSYS, where fluid flow was modeled by using the incompressible Navier-Stokes equations.

$$\begin{aligned} &\frac{\partial \rho_a}{\partial t} + \vec{\nabla}.\left(\rho_a V_a\right) = 0 \\ &\frac{\partial \rho_a \vec{V_a}}{\partial t} + \vec{\nabla}.\left(\rho_a \vec{V_a}\vec{V_a}\right) = \vec{\nabla}.\sigma^{ij} + \rho_a \vec{g} \\ &\vec{\nabla}.\left(\rho_a \vec{V_a} H_a\right) = \vec{\nabla}.\left(k_a \left(\vec{\nabla} T_a\right)^j + v_i \tau^{ij}\right) \end{aligned} \quad (1)$$

where σ^{ij} is the stress tensor, k is the thermal conductivity, E is the internal energy, τ is the shear stress and H is the enthalpy. C-type structured numerical grid was used, whereas to accurately determine the boundary layer characteristics (shear stresses and heat fluxes), a *y+* value less than 1 was used near the wall. The sand grain roughness height for the iced surface was calculated with an empirical NASA correlation described by Shin et al. [17, 20]. One equation and 2 equation turbulence models were tested and used as a compromise between acceptable computational cost and the required accuracy in simulating the turbulent flow. Two phase flow (air & water) was solved using Eulerian-Eulerian approach, where super cooled water droplets were assumed to be spherical. The Eulerian two phase fluid model consists of the Navier-Stokes equation, augmented by the water droplets continuity and momentum equation. The water droplet drag coefficient is based on the empirical correlation for the flow around the spherical droplets described by Clift et al. [21].

$$\frac{\partial \alpha}{\partial t} + \vec{\nabla}.\left(\alpha \vec{V}_d\right) = 0 \qquad (2)$$

$$\frac{\partial\left(\alpha \vec{V}_d\right)}{\partial t} + \vec{\nabla}.\left(\alpha \vec{V}_d.\vec{V}_d\right) = \frac{C_D \,\mathrm{Re}_d}{24K}\alpha\left(\vec{V}_a - \vec{V}_d\right) + \alpha\left(1 - \frac{\rho_a}{\rho_d}\right)\frac{1}{Fr^2}\vec{g}$$

$$K = \frac{\rho_d d^2 v_{a,\alpha}}{18 L_a U_a} \quad , \quad Fr = \frac{v_{a,\alpha}}{\sqrt{L_\alpha g}} \quad ,$$

$$\mathrm{Re}_d = \frac{\rho_d d v_{a,\alpha}\left\|v_a - v_d\right\|}{\mu_a}$$

where α is the water volume fraction, V_d is the droplet velocity, C_D is the droplet drag coefficient , K is the droplet inertia parameter and Fr is the Froude number. Surface thermodynamic and icing rate are calculated by Messinger Model using the mass and energy conservation equations, considering the heat fluxes due to convective cooling, evaporative cooling, heat of fusion, viscous heating, kinetic heating and solar radiation [22].

$$Q_{in}^{o} = Q_{out}^{o} \qquad (3)$$

$Q_{in} = Q_{\text{latent heat}} + Q_{\text{aerodynamic heat}} + Q_{\text{KE heat}}$

$Q_{out} = Q_{\text{sublimative heat}} + Q_{\text{convective heat}} + Q_{\text{droplet,cooling heat}} + Q_{\text{radiative heat}}$

$$Q_{sublimation} = \chi_s e_o (T_{surface} - T_{air})$$

$$\chi_s = \frac{0.622 h_c L_s}{C_p P_t L_e^{0.66}}$$

$$Q_{droplet,cooling} = \rho_a \beta v_\alpha C_{p,w} (T_{surface} - T_{air})$$

$$Q_{radiation} = 4\varepsilon\sigma_r T^3_{air} (T_{surface} - T_{air})$$

$$Q_{aerodynamic,heating} = \frac{r h_c v^2_\alpha}{2C_p}$$

$$Q_{latent,heat} = (LWC.\beta.v_\alpha).\left[L_f + C_i (T_{air} - T_{surface})\right]$$

$$Q_{droplrt,kinetic,energy} = (LWC.\beta.v_\alpha)\frac{v^2_\alpha}{2}$$

$$Q_{convection} = h_c (T_{surface} - T_{air})$$

where r is the adiabatic recovery factor, h_c is the convective heat transfer coefficient, c_i is the specific heat of ice, L_f is the latent heat of fusion, L_s is the latent heat of sublimation, L_e is the Lewis number and ε is the surface emissivity. ALE (Arbitrary Langrangian Eulerian) formulation was used for the mesh displacement due to ice accretion in time. This approach adds the grid speed terms to the Navier-Stokes equations to account for the mesh velocity[20].

ATMOSPHERIC ICING ON WIND TURBINE BLADE

Wind turbines are increasingly being planned and installed in cold areas like arctic and alpine, where they are periodically subject to atmospheric icing that effects their performance [23-25]. To study the ice accretion effect on performance of a wind turbine, a 63 m long NREL 5MW wind turbine blade [26] was selected as test case, mainly because availability of its geometric features and experimental data. 3D numerical analyses were carried out at different atmospheric icing conditions. Five sections were selected along the blade radius, where each section was 0.5 meter long. Figure-1 shows the selected blade sections and their locations along the blade radius.

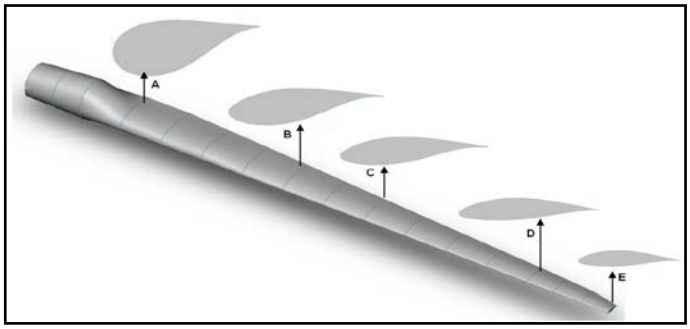

A	B	C	D	E
13.2 m	33.7 m	41.9 m	54.2 m	63 m

Figure 1 -Selected sections of NREL 5MW wind turbine blade

To study the rate and shape of ice accretion at different sections along the wind turbine blade, the numerical analyses were carried out for air and droplet velocity, v= 10 m/s, T= -10 C & t=60 min at α= 0. Results show that with the increase of

blade profile chord length and thickness and with the reduced air velocity, the relative size of the accreted ice reduces. Such decrease in the size of accreted ice is mainly due to the decrease in collection efficiency of the droplets with the blade and the reduction in velocity. Figure 2 shows the rate and shape of ice growth at each selected section, where black shaded area represents the accreted ice along blade section.

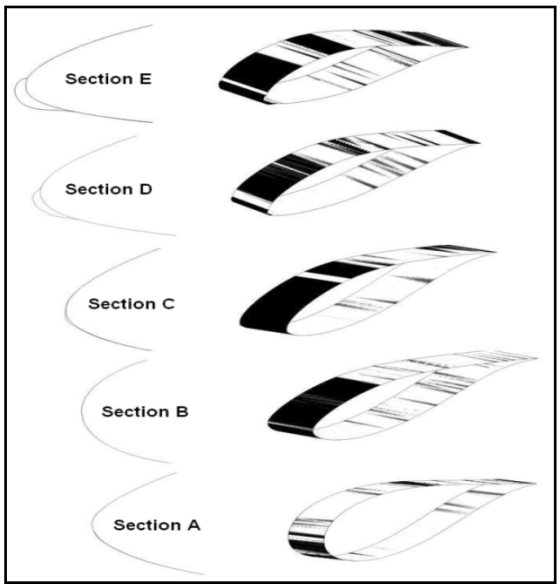

Figure 2- Ice accretion on selected sections of NREL 5MW wind turbine blade, T= -10C

Figure 3 shows that the value of accreted ice mass along blade. Results show that most affected area of the blade by ice is from tip to the center of the blade (from 30 m to 63 m), while rest of the area from blade center to the blade root is not having considerable effects of icing.

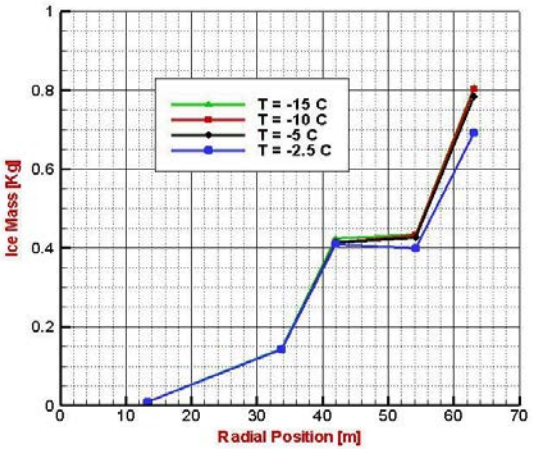

Figure 3- Accreted ice mass along blade surface at different operating temperatures

The numerical results were compared with the published data of NREL 5MW wind turbine and a good agreement was found. Figure 4 shows the power curves for the clean and iced NREL blade together with the curve published by NREL and a curve for what is called the improved iced case. The NREL curve is nearly indistinguishable from the clean (no ice) blade case. It can be seen that there is a significant power loss of about 27% because of the icing on over all rotor power.

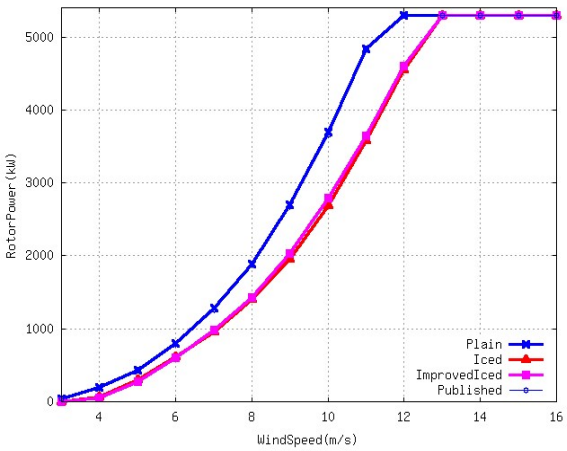

Figure 4- Performance comparison curve for clean and iced NREL 5MW wind turbine blade

ATMOSPHERIC ICE ON CIRCULAR OVERHEAD POWERLINE CONDUCTORS

The potential for damage to overhead power line conductor in cold regions as a result of atmospheric ice accretion is considerable. Llinca et al. [27] reported that large amplitude oscillations of ice covered cables at low frequencies is responsible for about one third of power line maintenance and operating cost. In this 2D numerical case study, the effect of ice accretion on circular power line conductors in tandem arrangement has been analysed at v = 10 m/s, T = -10C and t= 15 min. To validate the numerical model and understand the basics of ice accretion on power network cables, a simple circular cylindrical object is assumed initially and numerical analyses are validated with the experimental results obtained from the research paper of Ping Fu et al. [28]. Figure 5 shows the comparison between numerical and experimental results.

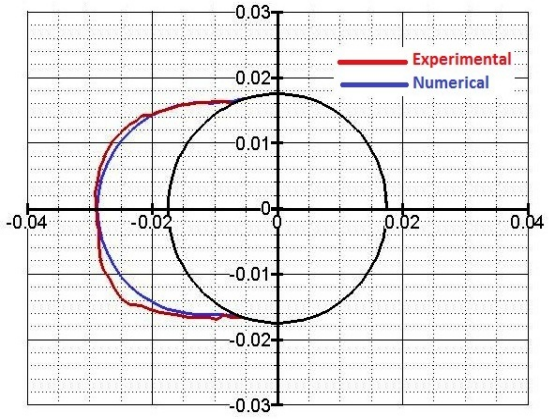

Figure 5-Comparison of accreted ice shape, obtained from numerical simulation with experiments.

Tandem arrangement of the circular overhead power line conductors has an effect on the ice accretion. Distance between conductors is one important factor in this regard, as it affects the airflow and droplet behavior. To analyze the effect of distance variation between two circular conductors in tandem arrangement, CFD based numerical analyses were carried out considering three different distance values (200, 400 & 600 mm).

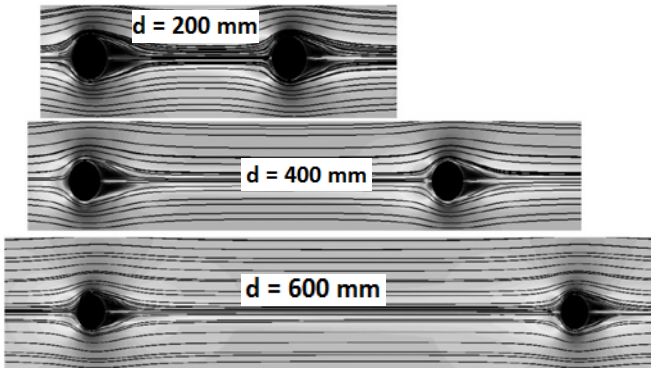

Figure 6- Velocity streamline around conductors

Results show a change in the air flow and droplet behavior with the change in the distance between conductors. With the increase in distance, the droplet collision efficiency on the rear conductor decreases, as more droplets follow the streamline after passing over the front conductor. In case of distance= 200 mm, after passing over the front conductor more droplets collide with the rear conductor surface due to the air flow behavior, as it does not get enough time to get settle, whereas in case of distance = 600 mm, air flow get settled before it reaches to the rear conductor.

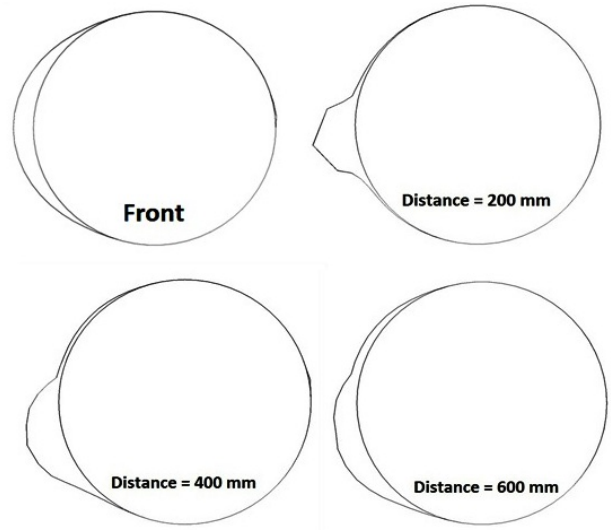

(Accreted Ice Shapes on conductors)

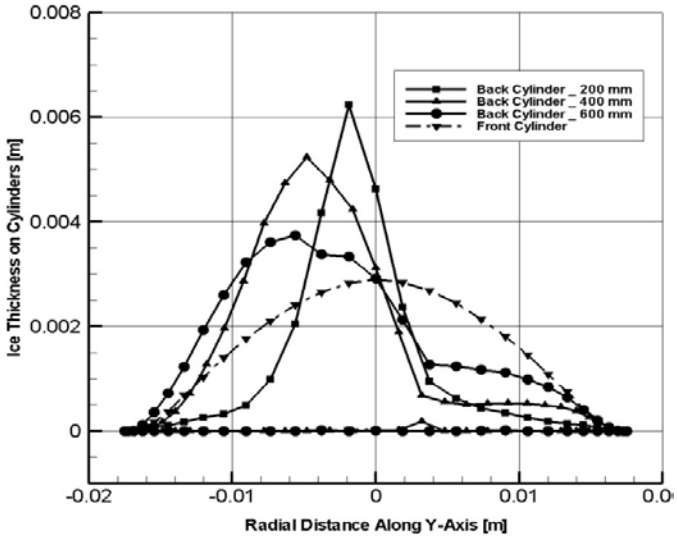

Figure 7- Effect of distance variation between conductors on rate and shape of accreted ice.

Figure-7 shows the ice accretion on both conductors in each case. Results show an abrupt ice shape on rear conductor in case of 200 mm because of air flow behavior, droplets do not collide evenly across the conductor surface and mainly collide at certain surface area, whereas in case of 600 mm results show a smooth ice shape at rear conductor due to settle flow behavior and even collision of droplets along the conductor surface. Such abrupt shapes of ice lead to aerodynamic instability of the power lines and can lead to severe damages. As an overall this numerical study showed a decrease in the accreted ice load and thickness with the increase of distance between circular power line conductors installed in the tandem arrangement.

Ice Accretion on Building's Air intake Louvers

In cold regions, air intake louvers on buildings are installed to shut out foreign matters like ice and snow particles to deflect, while allowing air to pass. In this case study a parametric numerical study has been carried out to numerically simulate the rate and shape of atmospheric ice accretion on louver slats. The analyses were carried out considering a louver structure with 7 slats, where distance between each slat is assumed 57 mm and placement angle of each slat is 45 degree. These 2D numerical analyses were carried out at v= 10 m/s, T = -10C, t = 15 min and α= 0.

Numerical analyses show the classical venturi effect in the vena contracta of the each louver slat. As air moves from larger corss section to smaller corss section of the louver slat, the corrosponding higer volume moves at a greater speed through the constriction. Air and water droplets are coupled with each other, therefore airflow behaviour effects the droplets movement along the surface. Results show the high droplet collison with the upper and front surface of the louvers, which leads to an increase in ice accretion along upper and front

surface of the louver slat. Figure-8 shows the air flow behaviour and resultant ice growth on the louver slats.

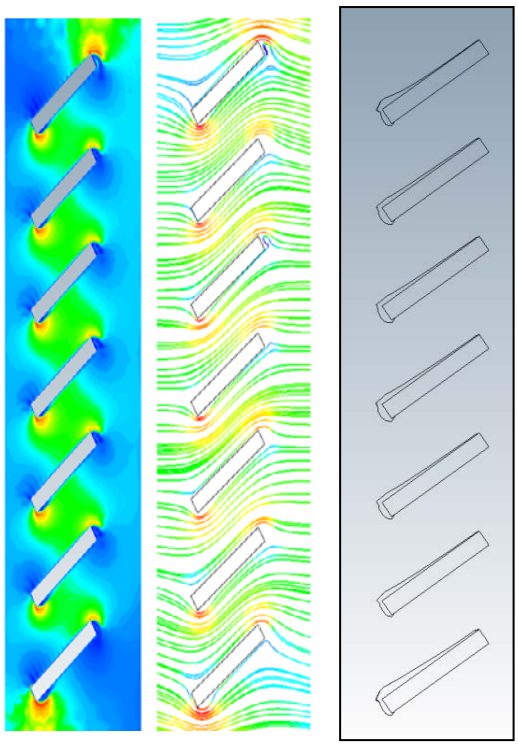

(Air Flow) (Ice Accretion)

Figure 8- Ice accretion on air intake louver slats

This numerical study provided the basic understanding of the ice accretion on louver slats and results showed that mainly ice accrets at front and top surface of the louver slats.

CONCLUSION

The analyses of above mentioned atmospheric ice related engineering applications showed that CFD is a mature and useful tool for modeling and evaluating such applications successfully. Three different study cases are discussed, where rate and shape of ice accretion was successfully numerically simulated on wind turbine blades, overhead power line conductors and buildings air intake louvers. A good agreement is found between numerical and experimental data; however appropriate knowledge and experience are very essential for obtaining reliable results.

ACKNOWLEDGEMENT

The work reported in this paper was partially funded by the Research Council of Norway, project no. 195153/160 and partially by the consortium of the project ColdTech-Sustainable Cold Climate Technology.

REFERENCES

1. T G Myers and J.P.F. Charpin., *A mathematical model for atmospheric ice accretion and water flow on a cold surface.* Heat & Mass Transfer, 2004. **47**: p. 5483-5500.
2. Kathleen F Jones and K.Z. Egelhofer, *Computer model of atmospheric ice accretion on transmission lines*.
3. Battan, I.J., *Cloud physics and cloud shedding*. 1962, New York: Doubleday and Co.
4. T Wagner, U. PEil, and C. Borri, *Numerical investigation of conductor bundle icing*, in *EACWE 5*2009: Florence, Italy.
5. S F Ackely and M.K. Templeton., *Computer modelling of atmopsheric ice accretion*, 1979, USA cold region research and engineering labortory.
6. E P Lozowski, J R Stallabrass, and F.P. Hearty., *The Icing of an unheated, Non-rotating Cylinder, Part I: A Simulation Model.* Journal of Climate and Applied Meteorology, 1983. **22**: p. 2053-2062.
7. E P Lozowski and M.M. Oleskiw, *Computer modelling of time dependant rime icing in the atmosphere*, 1983, USA cold regions research and engineering labortory.
8. E P Lozowski, K J Finstad, and E.M. Gates, *Comments on calculation of the impingement of cloud droplets on a cylinder by finite element method.* Journal of atmospheric science, 1985. **42**(3): p. 306-307.
9. McComber, P. *Numerical simulation of ice accretion on cables*. in *First international workshop on Atmospheric icing on structures*. 1983. Haniver, Hampshire.
10. McComber, P., R Martin, and G. Morin. *Estimation of combined ice and wind loads on overhead transmission lines.* in *First international workshop on atmospheric icing on structures*. 1983. Hanover, Hampshire.
11. B W Smoth and C.P. Barker. *Icing of cables*. in *First international workshop on atmospheric icing on structures*. 1983. Hanover, Hampshire.
12. Makkonen, L., *Models for the growth of rime, glaze, icicles and wet snow on structures.* Philosiphical transactions of the Royal Society A, 2000. **358**(1776): p. 2913-2939.
13. Makkonen, L., T. Laakso, and M. Marjaniemi, *Modelling and prevention of ice accretion on wind turbines.* Wind Engineering, 2001. **25**(1): p. 3-21.
14. Finstad, Lozowski, and Gates, *A computational investigation of water droplet trajectories.* Journal of atmospheric and ocenic technologies, 1988. **5**: p. 160-170.
15. Shin, J., *Prediction of ice shapes and their effect on airfoil drag.* Journal of aircraft, 1994. **31**(2): p. 263-270.
16. Boutanios, Z., *An Eulerian 3D analysis of water droplets impingement on a Convair-580 nose and*

cockpit geometry, in *Department of Mechanical Engineering*1999, Concordia University, Canada: Montreal.
17. J Shin and T.H. Bind., *Experimental and computational ice shapes and resulting drag increase for a NACA 0012 airfoil*, 1992, NASA technical memorandum 105743.
18. Skelton and Poots, *Snow accretion on overhead line conductors of finite torsional stiffness.* Cold region science and technology, 1991. **19**: p. 301-316.
19. http://www.newmerical.com/index.php/products/fensap-ice-cfd-software/.
20. Manual, N.S.U., 2010, NTI.
21. R Clift, J R Grace, and M.E. Weber, *Bubbles, Drops and Particles*. 1978, New York: Academic Press.
22. S O¨ zgen and Æ.M. Canıbek, *Ice accretion simulation on multi-element airfoils using extended Messinger model.* Heat Mass Transfer, 2009. **45**: p. 305-322.
23. Virk, M.S., M.C. Homola, and P.J. Nicklasson, *Effect of rime ice accretion on aerodynamic characteristics of wind turbine blade profiles.* Wind Engineering, 2010. **34**(2): p. 207-218.
24. Homola, M.C., et al., *The relationship between chord length and rime icing on wind turbines.* Wind Energy, 2009.
25. Matthew C Homola, et al., *Effect of atmospheric temperature and droplet size variation on ice accretion of wind turbine blades.* Journal of wind engineering and industrial aerodynamics, 2010. **In press**.
26. Jonkman, J., S. Butterfield, and W. Musial, *Defination of a 5 MW reference wind turbine for off shore system deveoplemnt*, 2009, National Renewable Energy Labortary, Technical report NREL/TP-500-38060. p. 75.
27. A Llinca, F Llinca, and L. Ignat. *Numerical study of iced conductor aerodynamics*. in *7th international workshop on atmospheric icing on structures*. 1996.
28. Ping Fu, Masoud Farzaneh, and G. Bouchard., *Two dimensional modelling of the ice accretion process on transmission line wires and conductors.* Cold region science & technology, 2006. **46**: p. 132-146.